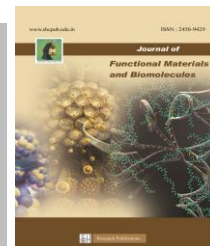




SACRED HEART RESEARCH PUBLICATIONS

Journal of Functional Materials and Biomolecules

Journal homepage: www.shcpub.edu.in



ISSN: 2456-9429

Electrical and ion transport studies on proton conducting polymer electrolyte poly (vinyl alcohol) - sulfamic acid

R. S. Daries Bella^a, R.S.Diana Sangeetha^b, G. Hirankumar^c

Received on 20 May 2021, accepted on 30 May 2021,
Published online on 21 June 2021

Abstract

Proton conducting solid polymer electrolytes comprised of poly (vinyl alcohol) (PVA) and sulfamic acid (SA) were prepared by a solution casting technique with different concentrations of SA. Surface morphology study showed the presence of aggregates in the solid polymer electrolytes doped with higher salt concentrations of SA. A complex formation between polymer and salt was confirmed by Fourier transformed infrared spectroscopy (FTIR). A detailed analysis of ac impedance studies suggested that the transport properties of the polymer complex were mainly affected by the aggregate formation. The nature of variation of dc conductivity with respect to temperature confirmed an Arrhenius behavior of the sample. The highest conductivity of $4.26 \times 10^{-7} \text{ S cm}^{-1}$ with low activation energy (1.02 eV) was observed for 97mol% PVA – 3mol% SA. The bulk resistance (R1) and constant phase element (CPE) of the polymer electrolyte were computed by the Z-view program. From equivalent circuit analysis, the roughness of the electrode-electrolyte interface was witnessed. The scaling behavior of the loss tangent spectra suggested that the dielectric relaxation mechanisms as a function of frequency describe the same conduction mechanism at different temperatures. Wagner's dc polarization measurement was used to find ionic transference number (0.99). The electrochemical stability window was measured by using Linear Sweep Voltammetry.

Keywords: Poly (vinyl alcohol), Sulfamic acid, Proton conductor, Polymer electrolytes, Dielectric relaxation, Impedance spectroscopy, Wagner's dc polarization Linear sweep voltammetry.

1 Introduction

Protons conducting solid polymer electrolytes have drawn much attention due to their potential applications in various electrochemical devices, such as Zn-air batteries, fuel cells, humidity sensors and electro chromic devices [1-10]. Though many proton conductors have been reported in the literature, the search for new, nontoxic, good thermal stability, high electrically conducting and good mechanical strength polymer electrolytes is still highly desirable. The presence of hydroxyl groups in the PVA involving the interchain hydrogen bond formation in the preparation of PVA by hydrolyzing the poly (vinyl acetate) has

been reported [11]. Biodegradable poly (vinyl alcohol) is a synthetic polymer used in wide range of industrial, commercial, medical and food applications [12, 13].

The conductivity of pure PVA at ambient temperature is reported to be $10^{-10} \text{ S cm}^{-1}$ [14, 15]. Although proton conducting polymer electrolytes based on PVA as host have been reported in the literature [14, 16], investigations are still being carried out to develop new proton conducting electrolytes based on PVA due to its biodegradable nature [17]. Hetero poly acids with PVA base polymer electrolytes act as a high solid state proton conductivity nearly 10^{-2} S/cm at room temperature due to fast proton hopping through conduction networks has been already reported [18]. Recently PVA doped with some inorganic alkali and alkaline earth metal salts like K, Mg and Li have been prepared and used as a various electrochemical device were reported [19-22]. Poly (vinyl alcohol) (PVA) has been the most widely used polymer host for Flexible Zinc – Air Batteries owing to its high chemical stability and simple fabrication process, was mechanically robust, exhibited good rechargeability and cycling stability and could be bent at different bending angles without any performance loss [23].

Sulfamic acid (SA) is one of the strong inorganic acids and it exhibits a zwitterionic form ($\text{NH}_3^+\text{SO}_3^-$) when in the solid state. SA has many applications in medical fields, materials engineering and industry. The growth, structure determination, dielectric and mechanical properties and UV-VIS, FTIR and Raman spectral studies of SA are already reported [24-27]. For instance, the conductivity of polyaniline was enhanced five orders of magnitude by doping with SA [24]. However, to our knowledge detailed ac impedance spectroscopic studies on poly (vinyl alcohol) doped with SA are unavailable in the literature. In the work described here, the effect of SA on the dielectric relaxation and conductivity behavior of PVA was studied.

*Corresponding author: e-mail darbelraj@gmail.com,

^a Department of Physics, Stella Maris College, Chennai, India

^b Department of Chemistry, Sacred Heart College, Tirupattur, Vellore. India

^c Department of Physics, Ramakrishna Mission Vivekananda College, Chennai, India

2 Experimental

2.1 Materials

Thin films of polymer electrolyte comprised of PVA (average Mw - 125,000 g/mol) (degree of hydrolysis = 88%) (SD Fine Chemical Ltd, India) and ionic dopant sulfamic acid ($\text{NH}_2\text{SO}_3\text{H}$) (FISCHER, 99%, India) were prepared with different weight ratios of PVA/SA (99mol%/ 1mol%, 98mol%/ 2mol%, 97mol%/ 3mol%, 96mol%/ 4mol%, 95mol%/ 5mol%) by a solution casting technique using distilled water as solvent.

2.2 Characterization

The laser microscopy image was recorded by using a Keyence VIC-9700 (Japan) with reflection mode. FTIR spectra were recorded for the polymer complexes using JASCO FTIR-4100 spectrometer in the wave number range of 400 cm^{-1} - 4000 cm^{-1} . The polymer electrolyte films were sandwiched between two aluminium electrodes and the AC impedance studies were carried out in the temperature range of 303K- 373K over the frequency range of 42Hz - 1MHz using a computer controlled Hioki 3532 LCR meter (Japan). Z View software was used to fit the experimental data of polymer electrolyte system to compute the bulk resistance and Constant Phase Element (CPE).

The ionic transference number of the mobile species in the polymer electrolyte was calculated by Wagner's dc polarization method. The electrochemical stability window of the polymer electrolytes was determined by means of linear sweep voltammetry using Biologic model SP-300 electrochemical work station with scan rate of 20mV/sec in the voltage range of 0-2V. Working and reference electrode used for this measurement were stainless steel and MnO_2 respectively with an area of 1 cm^2 .

3 Results and Discussion

3.1 Morphology analysis

The image of PVA and PVA-SA based polymer electrolyte membranes were observed by using optical microscopy. Figure 1a shows that the surface morphology of pure PVA, and Figure 1b, 1c, and 1d, 1e and 1f indicate that

1mol%, 2mol%, 3mol%, 4mol% and 5mol% SA doped cast polymer electrolyte films respectively and SA was dissolved into the PVA matrix and small size of crystallites of SA were found. But, for the highest salt concentration (Fig.1e and Fig.1f) of 4 and 5mol% of SA in 96 mol% and 95mol% of PVA, formation of crystallites or aggregates was detected. It has already been reported that the formation of zwitterions could only be observed when sulfamic acid exists in solid form [26].

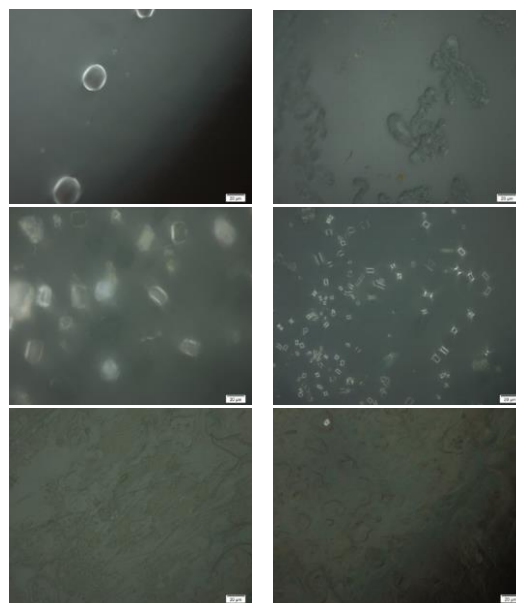


Figure 1. Laser microscopic images of a) pure PVA b) 1 mol% SA c) 2 mol% d) 3 mol% e) 4mol% f) 5mol% SA doped PVA.

3.2 Vibrational Analysis:

FTIR spectroscopy is an important tool to analyze the polymer electrolytes, since it gives information about interaction between the polymer and the ion. The vibrational bands of pure PVA and SA are as shown in tables 1.

Table 1: Vibrational bands and corresponding assignments of pure PVA and pure SA

Pure PVA Wave number (cm^{-1})	Assignments [28-30]	Pure SA Wave number (cm^{-1})	Assignments [26, 31]
810	Wagging of C-OH	683(s)	Stretching of N-S
832	Rocking of C-H	1005	Rocking of degen. NH_3^+
1025	Stretching of C-O	1060	Symmetric stretching of S=O
1094	Stretching of C-OH	1245	Asymmetric stretching of S=O
1241	Symmetric stretching of C-O	1439	Deformation of degen. NH_3^+
1265	Stretching of C-O-C	1538	Deformation of degen. NH_3^+
1330	Bending of C-H	2873	Symmetric stretching of NH_3^+
1374	Bending of C-H	3114	Stretching of degen. NH_3^+
1436(s)	Bending of C-H ₂		
1720	Stretching of C=O		
2912	Stretching of C-H		
2943(m)	Stretching of C-H		
3376	Stretching of OH		

FTIR spectra of PVA doped with different salts have been extensively studied using vibrational spectroscopic

techniques [28-30]. Figure 2 shows the FTIR spectra of pure PVA, $\text{NH}_2\text{SO}_3\text{H}$ and PVA doped with $\text{NH}_2\text{SO}_3\text{H}$.

The broad peak around 1720 cm^{-1} is due to C=O stretching of partially hydrolyzed PVA. It is worth mentioning that the PVA used in this study is 88% hydrolyzed. So, the remaining 12% contains the parent molecules of poly (vinyl acetate) (PVAc) as PVA is hydrolyzed from PVAc [30]. It is noticed that the addition of SA to PVA host polymer causes a new peak around 1660 cm^{-1} . The relative intensity of the new peak at 1660 cm^{-1} increases as increase in sulfamic acid concentration. The appearance of this new peak is due to the interaction of sulfamic acid with C=O of partially hydrolyzed PVA. The broad band around 1436 cm^{-1} that corresponds to the C-H bending of pure PVA is found to be shifted towards lower wave number. These changes in the wave number confirm the complex nature of the polymer electrolytes.

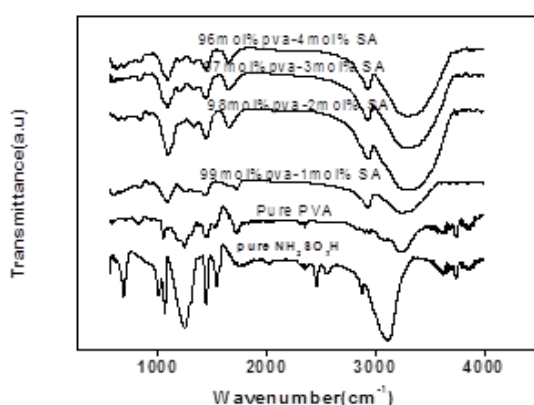


Figure 2. FTIR spectra of PVA-SA based polymer electrolyte

The peaks at 1441 cm^{-1} and 1538 cm^{-1} , which are attributed to N-H deformation mode of -NH_3^+ , are clearly visible for higher salt concentration (4mol% of SA). The existence of -NH_3^+ vibration is due to the zwitterionic formation of sulfamic acid [26]. The zwitterionic form of SA causes the formation of ion pairs and hence decrement of free ion concentration in the electrolytes.

N-H stretching vibrations are observed above 3200 cm^{-1} in the case of NH_2 whereas N-H stretching vibrations are observed below 3200 cm^{-1} in the case of -NH_3^+ in solid form of $\text{NH}_2\text{SO}_3\text{H}$ [19]. In the present work, the N-H stretching vibration of $\text{NH}_2\text{SO}_3\text{H}$ is noticed around 3110 cm^{-1} and hence the salt contains NH_3^+ vibrations. So, the band 3110 cm^{-1} also confirms the zwitterions formation of the salt [26, 31].

Moreover, the vibrational band situated at 1060 cm^{-1} and 1005 cm^{-1} impute the SO_3^- symmetric stretching and rocking mode vibration of -NH_3^+ respectively. The broad peak around 1245 cm^{-1} is due to OH bending vibrations of sulfamic acid. This vibrational band of $\text{NH}_2\text{SO}_3\text{H}$ is also affected when SA is dissolved in PVA. It is especially noticed that the SO_3^- stretching vibration of $\text{NH}_2\text{SO}_3\text{H}$ shifts towards lower wave number side in the polymer complex.

3.3 Conductivity analysis:

From a microscopic point of view, the ionic conductivity of a polymer electrolyte is given as $\sigma = nq\mu$, where n is number of charge carriers, q is the charge of the mobile carrier and μ is the mobility of the carrier. Figure 3 shows the variation of the logarithmic dc conductivity at 313K as a function of SA concentration expressed in its terms of mol%, the conductivity increased with increase of SA concentration up to 3mol%.

The increase of conductivity is due to the increase of mobile charge carriers, with all ions contributing to charge transport in the presence of the applied field. However, the conductivity decreases rapidly for 4mol% and then stayed approximately level for 5mol% of SA. The decrease is attributed to the formation of ion pairs which cannot move in the polymer matrix in the presence of an external electric field. These ion pairs are zwitterions of SA as confirmed by the laser microscopy results that showed the existence of un-dissociated salt at higher salt concentration which caused the decrease of conductivity.

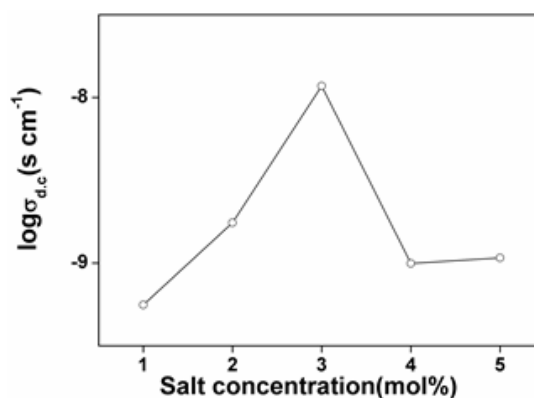


Figure 3. Variation of logarithmic dc conductivity with salt concentration at a temperature of 313K.

Table 2: Conductivity parameters of 3mol% of SA doped polymer electrolytes at various temperatures:

Temperature (K)	Resistance (R1) Ω	dc conductivity (S cm^{-1})	ω_p (rad s^{-1})	K ($\text{S cm}^{-1} \text{K rad}^{-1} \text{s}$)
313	1.03E6	1.17E-08	305	1.21E-08
323	2.95E5	4.10E-08	1425	0.93E-08
333	8.47E4	1.43E-07	5051	0.94E-08
343	2.84E4	4.26E-07	18353	0.80E-08
353	1.30E4	9.29E-07	40785	0.80E-08
363	7.29E3	1.66E-06	73999	0.81E-08
373	6.21E3	1.95E-06	86385	0.84E-08

3.4 Conductance spectra analysis

The variation of logarithmic ac conductivity with logarithmic angular frequency at different temperatures for 3mol% SA is shown in Figure 4; it shows two regions of ac conductivity up to the temperature of 333K: 1. frequency independent conductivity; i.e., dc conductivity in the low frequency region and 2. Frequency dependent conductivity; i.e., an ac dispersion region in the higher frequency region. The extrapolation of the frequency independent plateau to the y-axis at zero frequency provides the dc conductivity of the sample. The dc conductivity of 3mol% of SA at different temperatures is shown in the Table 2.

At higher frequencies, the conductivity shows a dispersion region that is attributed to correlated motions of the charge carriers. If the temperature is above 333K, low frequency dispersion is also observed. This low frequency dispersion is due to the accumulation of free ions at the electrode-electrolyte interface, i.e; space charge polarization. The cross over frequency, the frequency at which the dc conductivity regime changed into the ac conductivity dispersion region shifted towards higher frequencies region as the temperature is increased. The dc conductivity region is increased as the temperature increases (Figure 4) because of the enhanced mobility of the ions. Similar behavior is also observed for all other compositions.

The variation of dc conductivity with the inverse of temperature can be expressed in (inset Figure 4) using the Arrhenius equation,

$$\sigma T = \sigma_0 \exp(-E_a/kT)$$

where σ_0 is a pre-exponential factor, E_a is the activation energy, T is the absolute temperature in Kelvin and k is the Boltzmann constant. It is noted that logarithmic ionic conductivity linearly increases with decrease of $1/T$. From the slope of the straight line, the activation energy is calculated to be 1.02eV.

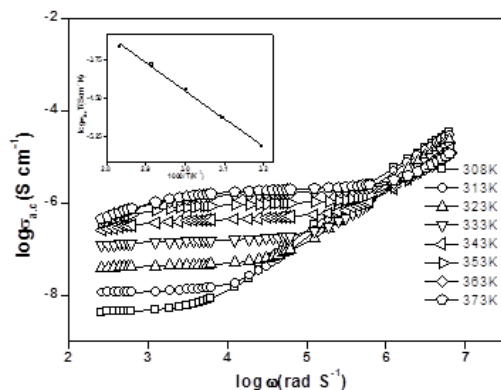


Figure 4. Conductance spectra for 3mol% SA doped PVA based polymer electrolytes. (Inset figure the variation of dc conductivity with the inverse of temperature)

3.5 Impedance analysis

Figure 5a shows typical Cole - Cole (Z' vs Z'') plot for 3mol% SA doped with 97mol% PVA polymer electrolyte at different temperatures. A depressed semicircle (inset) is observed only up-to the temperature of 323K; above 323K, the plot showed two well defined regions, namely, a de-

pressed semi circle in the high frequency region and an inclined, nearly straight line in the low frequency region. The depressed semicircle is due to the parallel combination of resistance and capacitance and the low frequency inclined straight line is due to the formation of an electrical double layer capacitance at the electrode-electrolyte interface. The inclined straight line and depressed semicircle indicate the distributed microscopic properties of the materials, which is represented by constant phase elements (CPE) [32-34].

A constant phase element represents an imperfect capacitor, i.e; a deviation from an ideal behavior. In an ideal case, an electrical double layer capacitance is represented by pure capacitor and the low frequency straight line appears parallel to the y-axis (Z'' axis) and the perfect semicircle is represented by a parallel combination of a resistor and capacitor. If any deviation from an ideal behavior (i.e., in the case of depressed semicircle or low frequency inclined straight line), the capacitors in an equivalent circuit are replaced by a constant phase element (CPE).

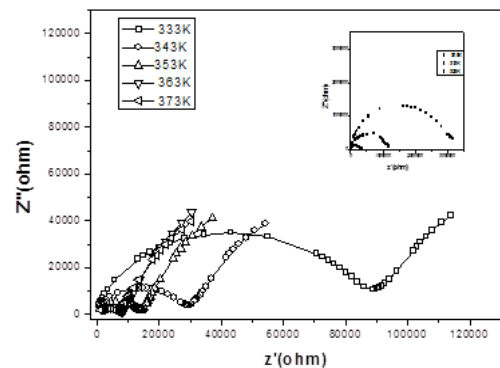


Figure 5 (a) Cole-Cole plots of 3mol% SA doped polymer electrolyte for different temperatures (inset: Cole-Cole plot for temperatures up to 323K)

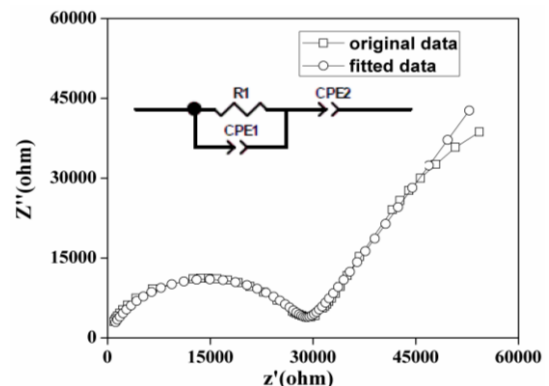


Figure 5(b) Fitted Cole-Cole plot of 3mol% SA doped PVA polymer electrolyte at 343K using Z view software (inset: its equivalent circuit).

Figure 5b shows the impedance plot of the 3mol% SA doped polymer electrolyte at 343K and the inset figure shows an equivalent circuit. The equivalent circuit represents the parallel combination of resistance R_1 and constant phase element CPE_1 followed by CPE_2 in series. Table 4 provides the values of some of the elements calculated.

ed by using the Z View software to fit the experimental data in Fig. 5b. The impedance of a CPE is expressed by $Z_{CPE}=1/C_d(j\omega)^\alpha$, where α is related to the deviation from the vertical of the line in the $-Z''$ vs Z' plot. $\alpha=1$ indicates a perfect capacitance and lower α values directly reflect the surface roughness of the electrode used [32, 34].

Table 3: Some elements computed by Z-view program using the equivalent circuit analysis for 3mol% of SA doped PVA polymer electrolyte at 343K

Elements	3mol% SA doped PVA polymer electrolyte	Unit
R1	28488	Ω
CPE1-T	7.59×10^{-10}	Farad
CPE1-P	0.83	No unit
CPE2-T	5.87×10^{-7}	Farad
CPE2-P	0.67	No unit

In the Z-view software, the CPE is expressed by two parameters CPE-T and CPE-P. CPE-T indicates the value of capacitance of the CPE elements. CPE1-P indicates the deviation from an ideal semicircle to the depressed semicircle and CPE2-P indicates the slope of the low frequency straight line [16]. The value of CPE2-P is 0.67 for 3mol% SA; being smaller than 1 indicates a rougher surface contact in the Al/Solid Polymer Electrolyte (SPE) /Al structure.

The presence of depressed semicircles also reveals the non- Debye nature of the sample. The bulk resistance, R1

was computed from the intercept of the semicircle on the low frequency side of the plot with the real axis. The bulk resistance (R1) decreased with increase of temperature (Table 3), which shows that the charge carriers were thermally activated.

3.6 Dielectric analysis

The complex dielectric permittivity, ϵ^* can be calculated by $\epsilon^* = \epsilon' - j \epsilon''$. where ϵ' is the real (relative permittivity or dielectric constant) and ϵ'' is the imaginary (dielectric loss) parts of the complex dielectric permittivity. The dielectric permittivity analysis provides information on the transport properties of ions in the electrolyte.

Figures 6 (a) and (b) show the plot between ϵ' vs. $\log \omega$ and ϵ'' vs. $\log \omega$ for 3mol% SA doped PVA at different temperatures, respectively. The real part of the permittivity measures the alignment of dipoles and the imaginary part represents the energy required to align the dipoles and to move ions [35]. The low frequency dispersion region of both spectra is due to the accumulation of charges at the electrode-electrolyte interface.

In the low frequency region, conductance losses predominated due to unavoidable electrode polarization. In the high frequency region, both spectra show decreasing magnitude that is saturated at very high frequency in the frequency range studied. This is due to the rapid, periodic reversal of field applied at the electrode-electrolyte interface which reduces the contribution of charge carriers to the dielectric permittivity.

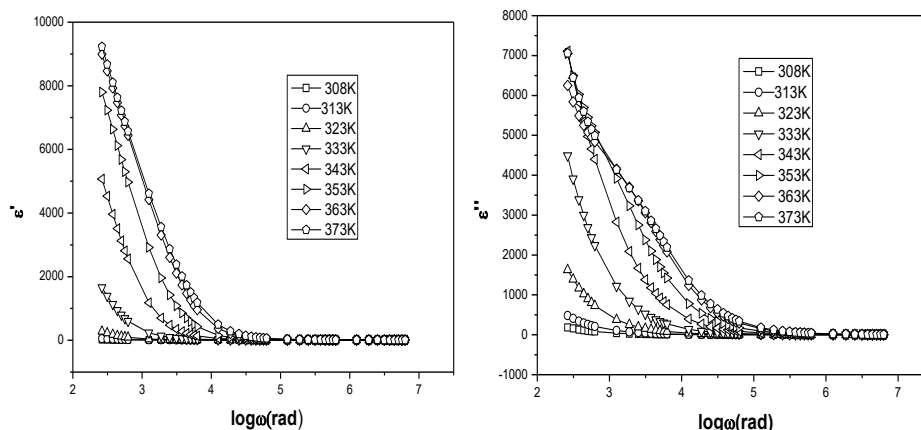


Figure 6 (a) Relative permittivity spectra **(b)** Dielectric loss spectra of 3mol% salt doped PVA based polymer electrolytes at various temperatures.

3.7 Dissipation factor analysis

The dielectric power loss is referred to the dissipation factor (D_e) or loss tangent ($\tan \delta$) and is given as $D_e = \epsilon''/\epsilon' = \tan \delta$. where δ is the loss angle. Figure 7 shows the angular frequency dependence of the $\tan \delta$ as a function of temperature for the 3mol% SA doped polymer electrolyte.

At each temperature, other than 308K and 313K, $\tan \delta$ was found to increase with increasing frequency and attained a maximum value ($\tan \delta_{max}$), then decrease with further increase of frequency. At low frequencies, the dipoles are able to keep in phase with the change of electric field and hence the power losses are low. As the frequency

is increased the dipole reorientation cannot be completed in the time available and the dipole become out of phase with the electric field and, hence, the power loss is maximum. The internal friction leads to the generation of heat. Further, the increase of frequency results in no time for substantial dipole movement, so the power losses are reduced. It is also observed that the maximum of $\tan \delta$ decreased with increase of temperature. This is attributed to increase in mobility of the chains at higher temperature, resulting in low power loss.

The angular frequency, ω_p , corresponding to $\tan \delta_{max}$ (Table 3), can also be used to calculate the activation ener-

gy for hopping of ions from the relation $\omega_p = \omega_e \exp(-E_m/kT)$ where ω_p - frequency of $\tan \delta_{\max}$ (hopping frequency), k is the Boltzmann's constant and T is an absolute temperature, ω_e is an effective attempt frequency. The inset in Fig.7 shows the temperature dependent logarithmic angular frequency.

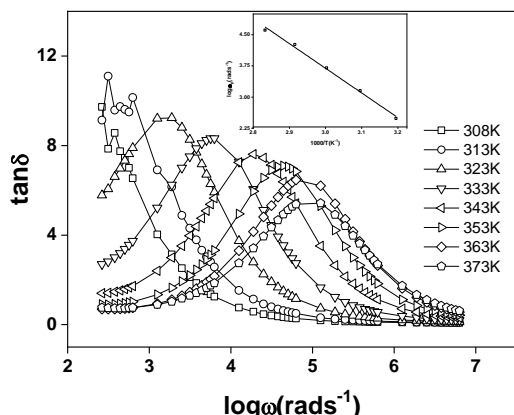


Figure 7. Variation of $\tan \delta$ with temperature for the 3mol% SA doped PVA based polymer electrolyte at different frequencies. (inset: shows the temperature dependent logarithmic angular frequency)

The activation energy, calculated from loss tangent ($E_m = 1.09$ eV, regression-0.983) is close to the dc conductivity activation energy (1.02eV) and implies that the creation of charge carriers is negligible in these systems i.e., the enthalpy of carrier formation can be neglected in these electrolytes [36].

The magnitude of the carrier concentration can be calculated from the formula $K = \sigma_{dc} T / \omega_p$ [37]. The values of the carrier concentration are tabulated in Table 3 for the various temperatures. The almost constant value of K shows that all energy is utilized for migration of ions.

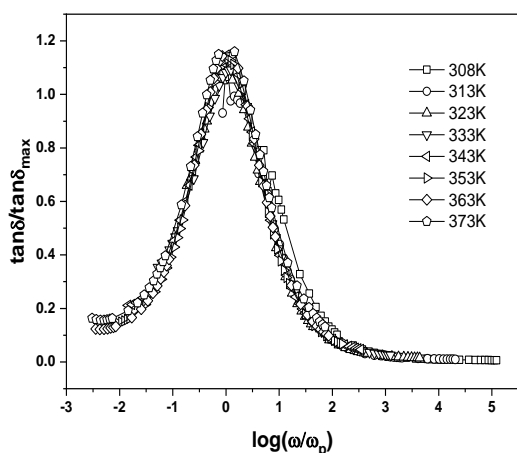


Figure 8. Normalized graph, $\tan \delta / \tan \delta_{\max}$, vs $\log(\omega/\omega_p)$ of the 3mol% SA doped PVA based polymer electrolyte at different temperatures.

Figure 8 shows the normalized graph of $\tan \delta / \tan \delta_{\max}$ vs $\log(\omega/\omega_p)$ at different temperatures. The normalized graph shows that all curves overlapped on a single master

curve. This implies that all possible relaxation mechanisms occurring at different frequencies exhibit the same thermal energy and the dynamical processes are temperature independent.

3.8 Wagner's dc polarization measurements

The ionic transference number i.e., the ratio of ionic conductivity to the total conductivity is an essential parameter to confirm the ionic motion in super ionic materials. The ionic transference number of the mobile species in the polymer electrolyte is calculated by Wagner's dc polarization method. The Wagner dc polarization method is found to be simple and effective method to analyze the ionic transference number measurements for ionic conductors [38]. Figure 9 shows the variation of polarization current as a function of time for 97mol% PVA-3 mol% SA. The ionic transference number is calculated from the plot using the standard equation. $t_{ion} = (I_i - I_f) / I_i$. Where I_i is the initial current due to the combination of ionic and electronic conduction and I_f is the final residual current due to electronic conduction.

The ionic transference number is found and the value is 0.99. This shows that the charge transports in these polymer electrolytes are mainly due to ions.

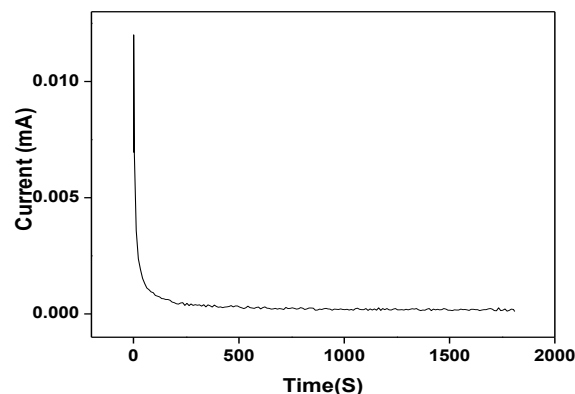


Figure 9. Ionic transference number for 97mol% PVA-3 mol% SA polymer electrolyte.

3.9 Linear Sweep Voltammetry

The electrochemical stability window measurement of the highest conducting solid polymer electrolyte (97 mol % PVA- 3 mol% SA) is performed to observe the ability of the polymer electrolyte to endure operating voltage of a battery system. This is obtained by linear sweep voltammetry experiment.

Figure 10 shows the linear sweep voltammogram of 97mol% PVA-3 mol% SA polymer electrolyte as a function of voltage. There is no obvious current through the working electrode from open circuit potential to 1.2 V, and then the current is increase that is related to the decomposition of the polymer electrolyte. The current is increased gradually when the electrode potential scans above 1.2 V. The decomposition potential for these polymer electrolytes is observed to be 1.5V. This result is higher than the reported in literatures [39, 40] for proton battery applications. But, result is lower than the value reported [41] in which re-

sult shows the electrochemical stability window of 1.8 V for polymer electrolyte film chitosan-NH₄NO₃-EC at room temperature with conductivity of $\sim 10^{-3}$ S cm⁻¹.

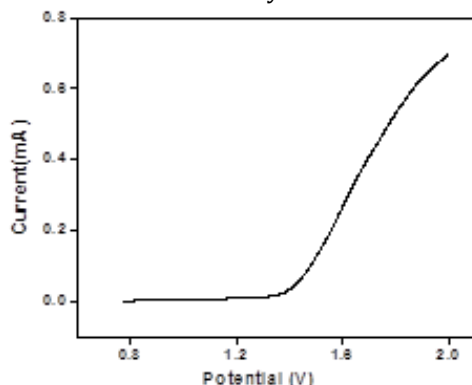


Figure 10. Linear sweep voltammogram of 97mol% PVA-3 mol% SA polymer electrolyte as a function of voltage.

4. Conclusion:

Proton conducting polymer electrolytes consisted of PVA - NH₂SO₃H with different compositions were prepared by a solution casting technique. Laser microscopic imaging witnessed the formation of aggregates/crystallites at higher salt concentrations. The complex formation between the polymer and the dissociated salt was confirmed from FTIR analysis. The highest dc conductivity was measured for 3mol% SA doped PVA, being 4.26×10^{-7} S cm⁻¹ at 343K. The temperature dependent conductivity was found to obey the Arrhenius law with activation energy of 1.02 eV.

The activation energy for conduction was found to be similar to the activation energy for migration of ions, calculated from the loss tangent, proving that the energy for charge carrier formation could be neglected in these electrolytes. An equivalent circuit analysis was used to study the roughness of the blocking electrode-electrolyte interface. The scaling of the loss tangent curves showed that the dielectric relaxation mechanism of these polymer electrolytes was independent of temperature. The ionic transport number confirmed that ionic conduction predominates in these types of electrolytes. LSV studies confirmed that the electrochemical stability window is about 1.5 V for polymer electrolyte and is in good agreement with the literature results.

Conflicts of Interest

The content, experimental data and the findings in this paper are original. It had no conflict of interest.

References

- [1] G.K. Surya Prakash, A. Federico Viva, Orianna Bretschger, Bo Yang, Moh El-Naggar, Kenneth Neilson, *J. Power Sources*, 195, 111-117 (2010).
- [2] R.S. Daries Bella, G. Hirankumar, Navanietha Krishnaraj, D. Prem Anand, *Materials Letters*, 164, 551-553 (2016).
- [3] S.K. Deraman, N.S. Mohamed, R.H.Y. Subban, *Int. J. Electrochem. Sci.*, 8, 1459 – 1468 (2013).
- [4] K. Naresh kumar, T. Sreekanth, M. Jaipal Reddy, U.V. Subba Rao, *J. Power Sources* 101, 130-133 (2001).
- [5] S.J. Peighambardoust, S. Rowshanzamir, M. Amjadi, *Int. J. Hydrogen Energy*, 35, 9349-9384 (2010).
- [6] M.F. Shukur, R. Ithnin, H.A. Illias, M.F.Z. Kadir, *Opt. mater.*, 35, 1834-1841 (2013).
- [7] G.Q. Zhang, X.G. Zhang, *Solid State Ionics* 2003, 160, 155–159.
- [8] E. George. Blomgren. *J. Power Sources* 1999, 81–82, 112–118
- [9] Weilin Xu, Changpeng Liu, Xinzhong Xue, Yi Su, Yanzhuo Lv, Wei Xing, Tianhong Lu, *Solid State Ionics*, 2004, 171,121-127.
- [10] H. Ohno, *Electrochim Acta*. 1992, 37, 1649-1651.
- [11] Anji Reddy Polua and Ranveer Kumar, *Chinese Journal of Polymer Science* Vol. 31, No. 4, (2013), 641–648.
- [12] M. Krumova, D. Lopez, R. Benavente, C. Mijangos, J.M.Perena.; *Polymer*, 2000, 41, 9265- 9272.
- [13] C.C. DeMerlis, D.R. Schoneker, *Food and Chemical Toxicology*, 2003, 41, 319-326
- [14] P.N. Gupta, K.P. Singh, *Solid State Ionics*, 1996, 86-88, 319-323
- [15] Rachna Mishra, K.J. Rao, *Solid State Ionics*, 1998, 106, 113-127
- [16] G. Hirankumar, S. Selvasekarapandian, N. Kuwata, J. Kawamura, T. Hattori, *J Power Sources*, 2005, 144, 262-267
- [17] C.S. Lim, K.H. Teoh, C.W. Liew, S. Ramesh, *Ionics*, 2014, 20, 251-258
- [18] Han Gao† and Keryn Lian, *J. Mater. Chem. A*, 2016, 4, 9585-9592.
- [19] Mayank Pandey, Girish M. Joshi, Narendra Nath Ghosh, *Int J Polym Mater*, 65, 2016 (15) 759 – 768.
- [20] Mangalam Ramaswamy, Tamilselvan Malayandi, Selvasekarapandian Subramanian, Jayakumar Srinivasalu, Manjuladevi Rangaswamy, Vairam Soundararajan. *Poly Plast Technol Eng*, 56, 2017 (9) 992 – 1002.
- [21] Sandeep Srivastava, Pradeep K. Varshney, *Int. J. Eng. Technol.*, 7 (2) (2018) 887-890.
- [22] Bashir Abubaker Abdulkadir, John Ojur Dennis, Muhammad Fadhullah Bin Abd. Shukur., Mahamed Mahmoud Elsayed Nasef, Fahad Usman, *Poly Plast Technol Eng*, 59, 2020 (15), 1679-1697.
- [23] Xiayue Fan, Jie Liu, Jia Ding, Yida Deng, Xiaopeng Han, Wenbin Hu, Cheng Zhong, *Front. Chem.*, 2019 (7), 678.
- [24] S. Ameen, V. Ali, M. Zulfequar, M. Mazharul Haq, M. Husain, *Curr Appl Phys*, 2007, 7, 215-219
- [25] R. RameshBabu, R. Ramesh, R. Gopalakrishnan, K. Ramamurthi, G. Bhagavannarayana, *Spectrochim Acta A*, 2010, 76, 470-475
- [26] D. Philip, A. Eapen, G. Aruldas, *J Solid State Chem*, 1995, 116, 217-223
- [27] F. A. Kanda, A.J. King, *J Am Chem. Soc.*, 1951, 73, 2315-2319.

- [28] S. Rajendran, M. Sivakumar, R. Subadevi, *Solid State Ionics*, 167, 2004,335-339
- [29] G. Hirankumar, S.Selvasekarapandian, M.S. Bhuvanewari, R. Baskaran, M. Vijayakumar, *J. Solid State Electrochem.*, 2006,10,193-197
- [30] M. Hema, S. Selvasekerapandian, G. Hirankumar, A. Sakunthala, D. Arunkumar, H. Nithya, *J. Physics and Chemistry of solids*, 2009,70, 1098-1103
- [31] R. Valluvan, K. Selvaraju, S. Kumararaman, *Mater. Chem. Phys*, 2006,97, 81-84
- [32] X. Qian, N. Gu, Z. Cheng, X. Yang, E. Wang, E. Dong, *Electrochem acta*. 2001, 46, 1829-1836
- [33] J. Ross Macdonald, (ed.) *Impedance Spectroscopy*, John Wiley and Sons, New York 1987, Chap.2
- [34] N. Hannachi, I. Chaabane, K. Guidara, K. A. Bulou, A. F. Hlel, *Mater Sci Engg B*. 2010, 172, 24-32
- [35] I. Ben Amor, H. Rekik, H. Kaddami, M. Raihane, M. Arous, A. Kallel, *J Electrostat*. 2009, 67, 717-722
- [36] E.F. Hairentidnov, N.F. Uvarov, *Phys. Rev. B*. 1994, 50, 13259-13266
- [37] D.P. Almond, A.R. West. *Soild State Ionics*, 1983, 9-10, 277-282.
- [38] J.B. Wagner, C.J. Wagner, *Chem. Rev.* 1957, 26, 1597-1601.
- [39] S.K. Deraman, N.S. Mohamed, R.H.Y.Subban, *Int. J. Electrochem. Sci.*, 2013,8, 1459 - 1468
- [40] R. Pratap, B. Singh, S. Chandra, *J. Power Sources*, 2006,161, 702-706
- [41] L.S. Ng, A.A. Mohamad, *Journal of Membrane Science*, 2008,325, 653-657